

See discussions, stats, and author profiles for this publication at: <https://www.researchgate.net/publication/279066879>

Pyrrolo-dC Metal-Mediated Base Pairs in the Reverse Watson-Crick Double Helix: Enhanced Stability of Parallel DNA and Impact of 6-Pyridinyl Residues on Fluorescence and Silver-Ion...

ARTICLE in CHEMISTRY - A EUROPEAN JOURNAL · JUNE 2015

Impact Factor: 5.73 · DOI: 10.1002/chem.201500582 · Source: PubMed

READS

20

3 AUTHORS, INCLUDING:



Hui Mei

University of California, Irvine

13 PUBLICATIONS 82 CITATIONS

SEE PROFILE

DNA Structures

Pyrrolo-dC Metal-Mediated Base Pairs in the Reverse Watson–Crick Double Helix: Enhanced Stability of Parallel DNA and Impact of 6-Pyridinyl Residues on Fluorescence and Silver-Ion Binding**

Haozhe Yang,^[a, b] Hui Mei,^[a, b] and Frank Seela^{*[a, b]}

Abstract: Reverse Watson–Crick DNA with parallel-strand orientation (ps DNA) has been constructed. Pyrrolo-dC (PyrdC) nucleosides with phenyl and pyridinyl residues linked to the 6 position of the pyrrolo[2,3-*d*]pyrimidine base have been incorporated in 12- and 25-mer oligonucleotide duplexes and utilized as silver-ion binding sites. Thermal-stability studies on the parallel DNA strands demonstrated extremely strong silver-ion binding and strongly enhanced duplex stability. Stoichiometric UV and fluorescence titration experiments

verified that a single ²pyPyrdC–²pyPyrdC pair captures two silver ions in ps DNA. A structure for the PyrdC silver-ion base pair that aligns 7-deazapurine bases head-to-tail instead of head-to-head, as suggested for canonical DNA, is proposed. The silver DNA double helix represents the first example of a ps DNA structure built up of bidentate and tridentate reverse Watson–Crick base pairs stabilized by a dinuclear silver-mediated PyrdC pair.

Introduction

Canonical DNA contains bidentate dA–dT and tridentate dG–dC Watson–Crick base pairs that induce an antiparallel-strand orientation of the double helix (aps DNA).^[1]

DNA with parallel strands (ps DNA) can be constructed by using dA–dT base pairs in the reverse Watson–Crick mode (Donohue pairs) and by replacing dG–dC base pairs with either 2'-deoxysoguanosine–dC (iG_d–dC) or 5-methyl-2'-deoxycytidine–dG (^miC_d–dG) pairs.^[2] Duplexes with parallel-strand orientation are resistant to nucleolytic enzymes, in particular to those enzymes that act on the double helix. The family of ps DNA forms an orthogonal pairing system, which shows unique properties with potential applications for antisense therapeutics, diagnostic purposes, or the formation of nanoscopic devices. Our laboratory and others have made significant contributions to the synthesis and application of ps DNA.^[3,4] Nevertheless, ps DNA is thermally less stable than canonical DNA. To overcome this problem, several protocols have been developed to stabilize ps DNA. An increase of the number of tridentate iG_d–dC or iC_d–dG pairs in ps DNA can counteract the loss

of stability by the dA–dT Donohue pairs.^[2c] Nucleoside shape mimics with a pyrrolo[2,3-*d*]pyrimidine or a pyrazolo[3,4-*d*]pyrimidine skeleton have been used to add additional stability to the parallel-helix structure.^[5] Also, the so-called “G-clamp” nucleoside and “click” cross-linking with bifunctional azides have been used for this purpose.^[6,7]

Some metal ions have the ability to bridge DNA base pairs, thereby strongly increasing the overall duplex stability because the bond energy of these base pairs is generally two or three times as high as that of protons in conventional base pairs. Additionally, metal ions can give the DNA molecule unique chemical and physical characteristics, including electrical conductivity, single-molecule magnetism, or charge-transfer properties.^[8] In aps DNA, a series of metal-mediated base pairs that add additional stability to the duplex structure has been investigated.^[9] Only recently, an extraordinary stable silver-ion-mediated base pair was reported for aps DNA. This metal base pair contains two pyrrolo-dC (PyrdC) ^[10] residues that can capture two silver ions and stabilizes DNA to the level of a covalent linkage (Figure 1 b).^[11,12] The PyrdC system is commonly used for sensitive DNA detection because the molecule exhibits fluorescence that communicates microenvironmental changes, such as hybridization, protonation, or metal binding.^[13–15] Five-membered heterocycles were introduced at the 6 position of the PyrdC moiety (systematic numbering is used)^[16] to improve the photophysical properties of the PyrdC system.

Up until now, very little has been known about the application of metal-mediated base pairs in ps DNA. Recently, cross-linked duplexes formed by dA–dT base pairs and containing one dC–dC metal pair^[17a] and a Hoogsteen duplex have been investigated.^[18] A study by Ono and co-workers^[17a] was limited to cross-linked DNA and the Hoogsteen DNA studied by Müller and co-workers^[18] was limited to certain purine-rich motifs and

[a] H. Yang, H. Mei, Prof. Dr. F. Seela
Laboratory of Bioorganic Chemistry and Chemical Biology
Center for Nanotechnology
Heisenbergstraße 11, 48149 Münster (Germany)
Fax: (+ 49) 251-53406857
E-mail: frank.seela@uni-osnabrueck.de

[b] H. Yang, H. Mei, Prof. Dr. F. Seela
Laboratorium für Organische und Bioorganische Chemie
Institut für Chemie neuer Materialien
Universität Osnabrück, Barbarastrasse 7, 49069 Osnabrück (Germany)

[**] dC = deoxycytidine.

Supporting information for this article is available on the WWW under <http://dx.doi.org/10.1002/chem.201500582>.

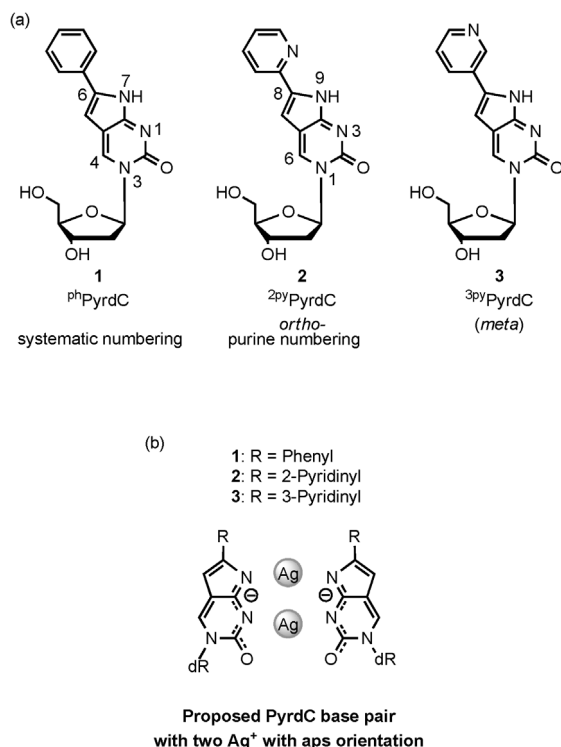


Figure 1. a) Structures of PyrdC derivatives and b) the proposed silver-mediated PyrdC–PyrdC base pair in aps duplexes. Ag corresponds to Ag⁺, dR = 2'-deoxyribofuranosyl.

required protonation of dC. However, both cases led to an increase of the duplex stability. So, it remains to be proven whether silver-mediated PyrdC–PyrdC base pairs can be formed in parallel reverse Watson–Crick DNA and how strongly the duplex is stabilized. Aps and ps DNA helices display distinct structural differences,^[19] such as the groove size and a reduced flexibility of the backbone of ps DNA (data not shown). Thus, the capability of ps DNA helix to accommodate a silver-mediated PyrdC–PyrdC base pair is not established.

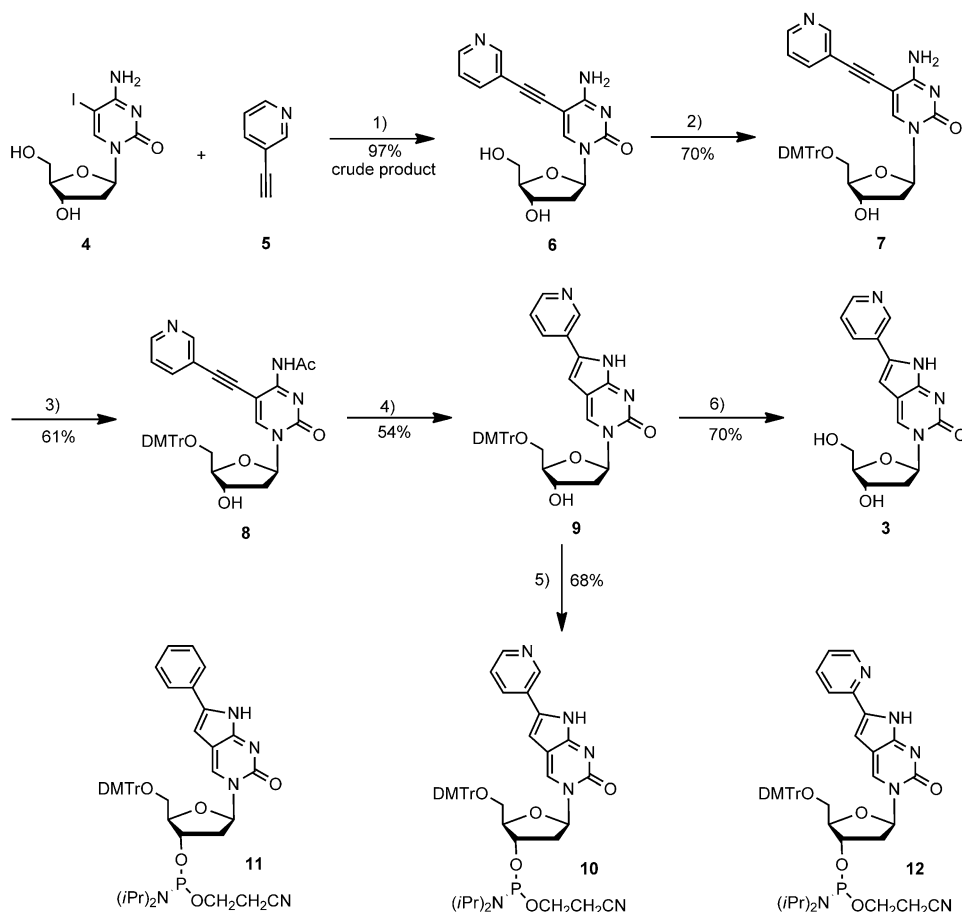
Herein, three different PyrdC nucleosides 1–3 with phenyl or pyridinyl residues at the 6 position (Figure 1a) were selected and introduced into ps DNA, and the formation of silver-mediated base pairs was evaluated. It was anticipated that the pyridinyl residues contribute ad-

ditional stability to the metal/base pairing system, and a significant difference was expected for the pyridine substituent with a nitrogen atom in the *ortho* or *meta* positions linked to the PyrdC skeleton (Figure 1b). Furthermore, the pyridinyl residues linked to the 6 position of the pyrrolo[2,3-*d*]pyrimidine moiety might enhance the fluorescence of the system.

Results and Discussion

Synthesis, characterization, and photophysical properties of nucleosides

The synthesis of 2pyPyrdC (2) has already been reported by our laboratory.^[11] Following this procedure, 3pyPyrdC (3) was synthesized in a similar way (Scheme 1). First, 5-(3-pyridinylethynyl)-dC (6) was obtained by a Sonogashira coupling of 5-iodo-2'-deoxycytidine (4)^[20] with 3-ethynylpyridine (5).^[21] The 4,4'-dimethoxytrityl (DMTr) residue was introduced at the 5' position to furnish 7. Because the direct annulation of the pyrrole system through the unprotected N4 amino group and the triple bond of the side chain often works inefficiently and leads to low yields, the amino group was protected before cyclization.^[10a] For this route, 7 was treated with acetic anhydride



Scheme 1. Synthesis of phosphoramidite 10. Reagents and conditions: 1) CuI, [Pd(PPh₃)₂Cl₂], Et₃N, DMF, 100 °C, 4 h; 2) 4,4'-dimethoxytriphenylmethyl chloride, anhydrous pyridine, (iPr)₂EtN, RT, 8 h; 3) acetic anhydride, DMF, RT, overnight; 4) CuI, Et₃N, DMF, 60 °C, 24 h; 5) NC(CH₂)₂OP(=O)(Cl)N(iPr)₂, (iPr)₂EtN, RT, 45 min; 6) dichloroacetic acid (2.5% in dry dichloromethane), Et₃N, 0 °C, 40 min.

in DMF, thus selectively yielding N4-acetyl-protected **8** (61 % yield). PyrdC derivative **9** was obtained in one step in the presence of CuI and triethylamine at 60 °C. Both deacetylation and cyclization proceeded simultaneously. The free pyrrolo-dC nucleoside ^{3py}PyrdC (**3**) was prepared by removing the DMT group of **9** in 2.5 % dichloroacetic acid/dichloromethane under standard conditions. Phosphitylation of **9** afforded the building block **10**. PyrdC phosphoramidites **11** and **12** were synthesized as previously reported.^[11,22]

All compounds were characterized by ESI mass-spectrometric and ¹H, ¹³C, and ³¹P NMR spectroscopic analysis. ¹H–¹³C gated-decoupled and DEPT-135 NMR spectra were used to assign the ¹³C NMR chemical shifts (Table 1; see the Experimental Section and Supporting Information for details).

PyrdC nucleosides exhibit fluorescence generated by the pyrrolo[2,3-*d*]pyrimidin-2-one system, which has been widely used to explore the structure and dynamics of nucleic acids.^[23] In earlier work, we used the fluorescence of PyrdC to study the formation of silver-mediated PyrdC–PyrdC base pairs in aps duplexes.^[12] Herein, the photophysical properties of **2** and **3** were determined in aqueous solution and methanol. The fluorescence spectra of **1–3** are shown in Figure 2 and the data are summarized in Table 2. The pyridinyl residues introduced at C6 of PyrdC improve the photophysical properties of **2** and **3** substantially (Table 2). Compounds **2** and **3** exhibit ten times higher quantum yields ($\Phi = 0.28$ – 0.34) relative to ^{me}PyrdC ($\Phi = 0.03$) in aqueous solution.^[24] Pyridinyl nucleosides **2** and **3** display an additional increase of the quantum yields in less polar methanol. Relative to the pyridine derivatives, phenyl nucleoside **1** is less sensitive to the change of solvent. The exceptionally high brightness values of **2** and **3** (3248 and 2938) relative to **1** (1894) result from the twofold higher extinction coefficients (Table 2). Similar observations were made by Tor and co-workers for thiophene derivatives.^[16] A redshift of the maxima of excitation is observed for **1–3** relative to the parent ^{me}PyrdC species, whereas the emission maxima are similar.

The Stoke shift of **1–3** ($\delta\lambda = 86$ – 96 nm) is smaller than that of ^{me}PyrdC (greater than $\delta\lambda = 110$ nm). Nevertheless, the excitation and emission maxima are far away from the UV absorption of DNA. Regarding the photophysical properties, the fluorescence data of nucleosides **2** and **3** are superior to ^{me}PyrdC and similar to the thiophenyl PyrdC derivative reported by Tor and co-workers.^[16]

As described later, the fluorescence changes of PyrdC-modified duplexes upon the addition of silver ions will be used to establish the stoichiometry of the silver/DNA complexes.

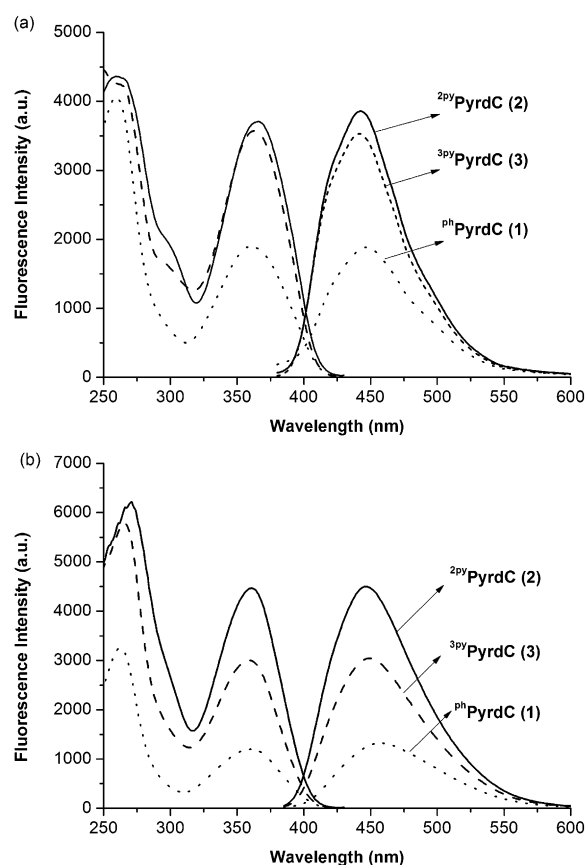


Figure 2. Fluorescence excitation and emission spectra of **1–3** recorded in a) methanol and b) buffer solution (100 mM NaOAc, 10 mM Mg(OAc)₂, 5 % DMSO, pH 7.4) at a concentration of 5 μ M. All compounds were excited at the maximum of excitation.

Therefore, the pK_a values of **2** and **3** were determined to evaluate the pH range in which the fluorescence is independent of pH value. The fluorescence decreases under both alkaline and acidic conditions (Figure 3). Within a pH range of 4–10, the fluorescence is independent of changes in the pH value and the neutral molecule is considered to be a fluorescent species.

The pK_a values of protonation ($pK_a = 3.0$ and 4.1 for **2** and **3**, respectively) are tentatively assigned to the protonation of N1 (systematic numbering). The pK_a values of deprotonation for **2** and **3** are similar ($pK_a = 11.1$ and 11.0 for **2** and **3**, respectively), with reference to the deprotonation of the pyrrole moiety. A similar pK_a value was reported for ^{ph}PyrdC ($pK_a = 11.5$)^[25] in which there is a phenyl instead of a pyridinyl residue attached

Table 1. ¹³C NMR chemical shifts (δ) of PyrdC nucleosides.^[a]

| Cmpound | C2 ^[b] /C2 ^[c] | C6 ^[b] /C6 ^[c] | C5 ^[b] /C4a ^[c] | C5 ^[c] | C6 ^[c] | C4 ^[b] /C7a ^[c] | C1' | C2' | C3' | C4' | C5' | OMe | C≡C | pyridinyl |
|----------|--------------------------------------|--------------------------------------|---------------------------------------|-------------------|-------------------|---------------------------------------|------|------|------|------|------|------|------------|-----------------------------------|
| 6 | 153.3 | 145.4 | 90.6 | – | – | 163.7 | 85.5 | 40.8 | 69.8 | 87.4 | 60.8 | – | 84.9, 88.9 | 119.6, 123.3, 138.2, 151.5, 153.3 |
| 7 | 153.1 | 144.4 | 90.7 | – | – | 163.6 | 85.7 | 41.1 | 70.4 | 85.9 | 63.4 | 54.8 | 84.1, 89.3 | 119.3, 122.9, 138.0, 148.3, 151.3 |
| 8 | 152.4 | 147.0 | 93.0 | – | – | 161.0 | 87.2 | 41.2 | 69.9 | 86.5 | 63.1 | 54.9 | 83.7, 91.7 | 119.2, 123.1, 138.1, 148.7, 151.3 |
| 9 | 153.4 | 145.7 | 108.4 | 97.6 | 135.8 | 159.6 | 86.5 | 41.1 | 68.7 | 85.4 | 62.2 | 54.7 | – | 123.6, 126.2, 131.6, 136.5, 148.7 |
| 3 | 153.9 | 146.2 | 108.9 | 98.6 | 136.3 | 159.9 | 87.2 | 41.5 | 69.8 | 88.0 | 60.9 | – | – | 123.9, 126.7, 132.2, 136.3, 149.0 |

[a] Measured in [D₆]DMSO at 298 K. [b] Pyrimidine numbering. [c] Systematic numbering.

Table 2. Photophysical properties of PyrdC nucleosides.^[a]

| Compound | λ_{max} [nm] | ϵ [mol ⁻¹ dm ³ cm ⁻¹] | $\lambda_{\text{ex, max}}$ [nm] | $\lambda_{\text{em, max}}$ [nm] | Quantum yield (Φ) ^[b] | Brightness ^[c] |
|------------------------------------|-----------------------------|--|---------------------------------|---------------------------------|---|---------------------------|
| 1 | 360 (364) | 5920 (6000) | 361 (360) | 457 (448) | 0.32 (0.28) ^[d] | 1894 (1680) |
| 2 | 362 (367) | 11 600 (13 300) | 361 (366) | 447 (443) | 0.28 (0.37) | 3248 (4921) |
| 3 | 359 (366) | 8640 (12 100) | 360 (362) | 449 (442) | 0.34 (0.41) | 2938 (4961) |
| ^{me} PyrC ^[d] | 344 | 3100 | 336 ^[e] | 450 ^[e] | 0.06 ^[e] | 186 ^[e] |
| ^{me} PyrdC ^[d] | 340 | 3500 | 341 | 457 | 0.03 | 105 |

[a] UV and fluorescence spectra were measured in buffer solution (100 mM NaOAc, 10 mM Mg(OAc)₂, 5% DMSO, pH 7.4) and methanol (data in parentheses). [b] Quantum yields were determined with quinine sulfate in 0.1 N H₂SO₄ as a standard with $\Phi = 0.54$. [c] The brightness was calculated as: brightness = $\epsilon \cdot \Phi$. [d] Data were taken from references [14] and [24]. ^{me}PyrC = 6-methylpyrrolocytidine, ^{me}PyrdC = 6-methylpyrrolo-2'-deoxycytidine. [e] Determined in 0.5% DMSO/H₂O.

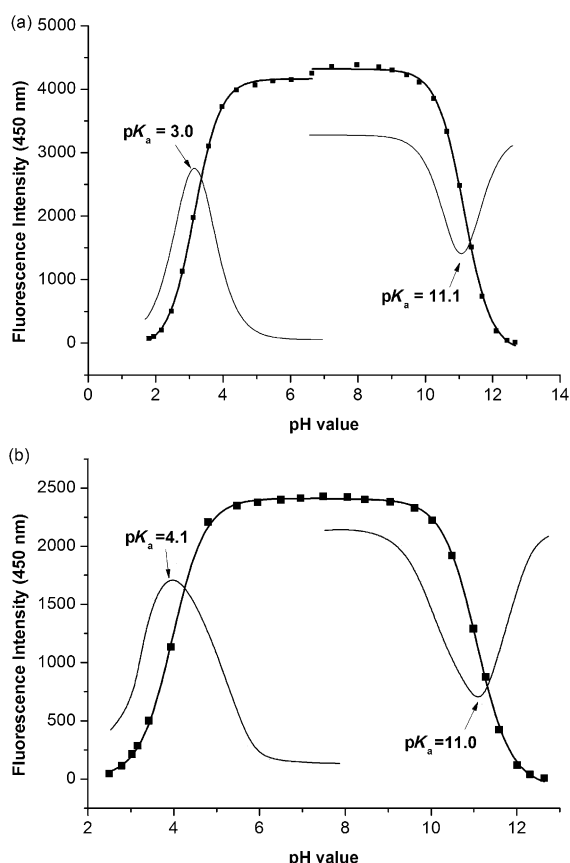


Figure 3. Graphs of fluorescence-emission intensity versus pH value. a) ^{2py}PyrdC (10 μ M) and b) ^{3py}PyrdC (5 μ M) at $\lambda = 450$ nm ($\lambda_{\text{ex}} = 362$ nm). Measurements were performed in 0.1 M sodium phosphate buffer solution (see the Supporting Information for details).

to the 6 position. Taken together, PyrdC derivatives **1–3** are highly fluorescent under near neutral conditions.

Oligonucleotide synthesis and characterization

Next, the pyrrolo-dC derivatives ^{ph}PyrdC (**1**), ^{2py}PyrdC (**2**), and ^{3py}PyrdC (**3**) were incorporated into the center of 12- and 25-mer oligonucleotides (Table 3). The corresponding phosphoramidites **10–12** and the standard building blocks were employed in solid-phase oligonucleotide synthesis. The phosphor-

amidites of 2'-deoxyisoguanosine iG_d **13** and 5-methyl-2'-deoxyisocytidine ^{me}iC_d **14** were used in place of dG and dC to construct oligonucleotides ODN-**2** and ODN-**5** (see Table 3 and Figure S1 in the Supporting Information).

PyrdC-containing oligonucleotides are labile under harsh deprotection conditions (aq. NH₃, 60 °C, overnight). Consequently, these derivatives were deprotected in 25% aqueous NH₃ at

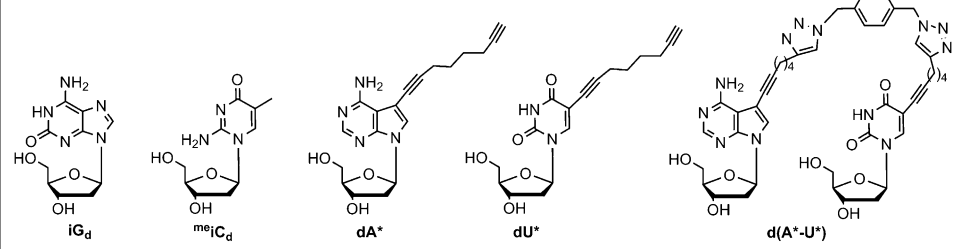
60 °C for 1 hour and kept at room temperature overnight. ODN-**2** and ODN-**5** containing iG_d and ^{me}iC_d modifications were kept in 25% aqueous NH₃ at room temperature for 2 days. Complete deprotection of all oligonucleotides was confirmed by mass-spectrometric analysis (Table 3). The oligonucleotides were purified before and after detritylation by using reversed-phase HPLC (RP-18), and the purity of the oligonucleotides was confirmed also by using RP-HPLC (see Figure S4 in the Supporting Information), and the composition of the PyrdC-modified oligonucleotides was verified by using MALDI-TOF mass spectrometry. Other oligonucleotides displayed in Table 3 had already been described.^[5a,6,11,12]

PyrdC base pairs in ps DNA in the presence and absence of silver ions

The unique structure of the ps double helix shows a number of properties similar to aps DNA, as well as many differences. According to NMR spectroscopic measurements and modeling studies, the orientation of the nucleobase in ps DNA is anti and the sugar conformation is in the S-domain, similar to aps DNA. The diameter of the right-handed helix is almost the same for ps and aps DNA (20 Å), whereas the helical parameters of ps and aps DNA are different, thus leading to two grooves with an almost identical widths of 8–9 Å for ps DNA relative to widths of 6 and 12 Å in aps DNA. The interstrand C1'...C1' distance of ps DNA (ca. 11.4 Å) is 2 Å larger than in aps DNA.^[19,32]

With this study, we demonstrate that silver-mediated PyrdC–PyrdC base pairs can also be formed in parallel duplexes, thereby leading to strong duplex stabilization. The thermal stability of 12-mer duplexes with PyrdC hetero and homo base pairs was determined by the *T_m* measurement monitored by changes in UV absorption in the presence and absence of silver ions. The experiments were performed on ps DNA and compared to duplexes with an aps orientation. The *T_m* values are summarized in Tables 4 and 5. In all cases, the melting profiles of silver-free and silver-saturated (with 2 equiv of Ag⁺ ions) duplexes show typical sigmoidal transitions similar to the reference duplexes. With a shortfall of silver ions (1 equiv of Ag⁺ ions per base pair), a few duplexes show biphasic melting (Figure 4).^[11] The lower *T_m* value derived from the biphasic melting refers to the silver-free duplex, whereas the higher

Table 3. Oligonucleotides used in this study and their molecular masses.

| 12-mer Oligonucleotides | | Calcd $[M+H]^+$ | Found $[M+H]^+$ [a] |
|--|----------|-----------------|---------------------|
| 5'-d(TICA TAA 2TiG iGAT) | (ODN-2) | 3760.5 | 3759.5 |
| 5'-d(TICA TAA 3TiG iGAT) | (ODN-5) | 3760.5 | 3761.0 |
| 3'-d(TCA TAA 3TG GAT) | (ODN-6) | 3744.8 | 3745.1 |
| 5'-d(AGT ATT 3AC CTA) | (ODN-11) | 3706.5 | 3704.9 |
| 12-mer Oligonucleotides [b] | | | |
| 5'-d(AGT ATT CAC CTA) | (ODN-1) | | |
| 3'-d(TCA TAA 2TG GAT) | (ODN-3) | | |
| 5'-d(AGT ATT GAC CTA) | (ODN-4) | | |
| 5'-d(AGT ATT 1AC CTA) | (ODN-7) | | |
| 3'-d(TCA TAA 1TG GAT) | (ODN-9) | | |
| 5'-d(AGT ATT 2AC CTA) | (ODN-10) | | |
| 5'-d(TAG GTC AAT ACT) | (ODN-12) | | |
| 5'-d(ATiC iCAiG TTA TiGA) | (ODN-13) | | |
| 25-mer Oligonucleotides | | Calcd $[M+H]^+$ | Found $[M+H]^+$ [a] |
| 5'-d(A*AA AAA AAA ATA ATT TTA AAT ATTT) | (ODN-14) | 7790.3 | 7790.2 |
| 5'-d(U*TT TTT TTT TAT TAA AAT TTA TAAA) | (ODN-15) | 7714.2 | 7714.5 |
| 5'-d(AAA AAA AAA ATA 1TT TTA AAT ATTT) | (ODN-16) | 7764.2 | 7761.6 |
| 5'-d(TTT TTT TTT TAT 1AA AAT TTA TAAA) | (ODN-17) | 7710.2 | 7707.7 |
| 5'-d(AAA AAA AAA ATA 2TT TTA AAT ATTT) | (ODN-18) | 7765.2 | 7764.8 |
| 5'-d(TTT TTT TTT TAT 2AA AAT TTA TAAA) | (ODN-19) | 7711.2 | 7710.3 |
| 5'-d(AAA AAA AAA ATA 3TT TTA AAT ATTT) | (ODN-20) | 7765.2 | 7763.0 |
| 5'-d(TTT TTT TTT TAT 3AA AAT TTA TAAA) | (ODN-21) | 7711.2 | 7709.1 |
| 3'-d(TTT TTT TTT TAT 1AA AAT TTA TAAA) | (ODN-24) | 7710.2 | 7709.4 |
| 3'-d(TTT TTT TTT TAT 2AA AAT TTA TAAA) | (ODN-25) | 7711.2 | 7710.2 |
| 3'-d(TTT TTT TTT TAT 3AA AAT TTA TAAA) | (ODN-26) | 7711.2 | 7709.9 |
| 5'-d(A*AA AAA AAA ATA ATT TTA AAT ATTT) | (ODN-28) | 15692.7 | 15693.6 |
| 5'-d(U*TT TTT TTT TAT TAA AAT TTA TAAA) | | | |
| 25-mer Oligonucleotides [b] | | | |
| 5'-d(AAA AAA AAA ATA ATT TTA AAT ATTT) | (ODN-22) | | |
| 5'-d(TTT TTT TTT TAT TAA AAT TTA TAAA) | (ODN-23) | | |
| 3'-d(TTT TTT TTT TAT TAA AAT TTA TAAA) | (ODN-27) | | |
|  | | | |

[a] Determined by MALDI-TOF mass-spectrometric as the $[M+H]^+$ ion in the linear positive mode. [b] Oligonucleotides of existing and characterized samples. [5a,6,11,12] $iC_d = meIc_d$

T_m value refers to the duplex that captures two silver ions. These two species coexist in solution, and no T_m value for species that bind one silver ion was detected. When two equivalents of silver ions were added, only the higher T_m value was observed (monophasic melting). Thus, it is obvious that the PyrdC–PyrdC base pair instantaneously captures two silver ions in a cooperative way. Cooperative metal-ion binding for copper ions has already been discussed by Clever and Shionoya^[9b] and Müller and co-workers.^[33] Nevertheless, the situation that causes cooperative metal binding is different to our experiments. In our case, two silver ions are bound to the same PyrdC–PyrdC base pair. The cooperative binding of silver ions between two silver-mediated base pairs reported by

Müller and co-workers occurred in a nearest-neighbor situation.

In our experiments, the addition of silver ions leads to slight hypochromicity changes that are more pronounced in aps than in ps DNA.

PyrdC–dG and PyrdC–dC hetero base pairs in 12-mer DNA in the presence and absence of silver ions

In the first series of experiments, the pairing properties of the PyrdC derivatives 1–3 against dG (matching base pair) in aps DNA were investigated in the presence and absence of silver ions. In all cases, stabilized duplexes were formed when dC was replaced by the PyrdC derivatives 1–3 ($\Delta T_m = +3.5$ – 5.5 °C), possibly by increased stacking interactions of the pyrrolo[2,3-*d*]pyrimidine system. The addition of silver ions has no obvious effect on the duplex stability, thus indicating that canonical base pairs are not stabilized by silver ions (Table 4).

The formation of ps duplexes containing PyrdC–dC base pairs was then studied in the absence and presence of silver ions and compared to the corresponding aps duplexes. The capture of one silver ion by the PyrdC–dC pair has already been reported for aps DNA.^[15] For the first time, this base pair has been investigated in the context of ps DNA.

The PyrdC–dC base pairs cause a significant decrease in

T_m value (mismatch formation) both in ps and aps duplexes (Table 4). The addition of one equivalent of silver ions induces a notably increase of the ps-duplex stability ($\Delta T_m = +7.0$). No substantial increase in T_m value was found by further addition of silver ions for PyrdC derivatives 1–3. This finding demonstrates that each PyrdC–dC base pair also captures only one silver ion in ps DNA, as reported for the aps duplexes.

PyrdC–PyrdC base pairs in 12-mer duplex DNA in the presence and absence of silver ions

Encouraged by the results of the aforementioned experiments, the formation of silver-mediated PyrdC–PyrdC homo and

Table 4. T_m values of 12-mer DNA duplexes containing PyrdC–dG and PyrdC–dC hetero base pairs in the presence and absence of silver ions.^[a]

| | | T_m [°C] with n equiv of AgNO ₃ | | | ΔT_m [°C] ^[b] |
|---------------------------|----------|--|---------------------|---------------------|----------------------------------|
| | | $n=0$ | $n=1$ | $n=2$ | |
| aps duplexes | | | | | |
| 5'-d(AGT ATT GAC CTA) | (ODN-4) | 46.5 | 47.0 | 46.5 | +0 |
| 3'-d(TCATAA CTG GAT) | (ODN-12) | | | | |
| 5'-d(AGT ATT GAC CTA) | (ODN-4) | 50.5 | n.d. | 48.0 | −2.0 |
| 3'-d(TCA TAA 1TG GAT) | (ODN-9) | | | | |
| 5'-d(AGT ATT GAC CTA) | (ODN-4) | 50.0 ^[c] | 50.0 ^[c] | 48.0 ^[c] | −2.0 ^[c] |
| 3'-d(TCA TAA 2TG GAT) | (ODN-3) | | | | |
| 5'-d(AGT ATT GAC CTA) | (ODN-4) | 52.0 | n.d. | 52.5 | +0.5 |
| 3'-d(TCA TAA 3TG GAT) | (ODN-6) | | | | |
| 5'-d(AGT ATT CAC CTA) | (ODN-1) | 33.0 ^[c] | 35.5 ^[c] | 36.5 ^[c] | +3.5 |
| 3'-d(TCA TAA 1TG GAT) | (ODN-9) | | | | |
| 5'-d(AGT ATT CAC CTA) | (ODN-1) | 30.5 | 36.5 | 36.0 | +5.5 |
| 3'-d(TCA TAA 2TG GAT) | (ODN-3) | | | | |
| 5'-d(AGT ATT CAC CTA) | (ODN-1) | 31.5 | 36.0 | 37.0 | +5.5 |
| 3'-d(TCA TAA 3TG GAT) | (ODN-6) | | | | |
| ps duplexes | | | | | |
| 5'-d(TAG GTC AAT ACT) | (ODN-12) | 34.5 | n.d. | 33.5 | −1.0 |
| 5'-d(ATiC iCAiG TTA TiGA) | (ODN-13) | | | | |
| 5'-d(AGT ATT CAC CTA) | (ODN-1) | 23.0 | 30.0 | 30.0 | +7.0 |
| 5'-d(TiCA TAA 2TiG iGAT) | (ODN-2) | | | | |
| 5'-d(AGT ATT CAC CTA) | (ODN-1) | 24.0 | 31.0 | 30.0 | +6.0 |
| 5'-d(TiCA TAA 3TiG iGAT) | (ODN-5) | | | | |

[a] Measured at $\lambda = 260$ nm with $5 \mu\text{M} + 5 \mu\text{M}$ single-strand concentration at a heating rate of $1.0^\circ\text{C min}^{-1}$ in buffer solution (100 mM NaOAc, 10 mM $\text{Mg}(\text{OAc})_2$, pH 7.4) in the presence of various concentrations of AgNO_3 (0–2.0 equiv.). T_m values were calculated from the heating curves. [b] $\Delta T_m = T_m(\text{after addition of 2 equiv } \text{AgNO}_3) - T_m(\text{before addition of } \text{AgNO}_3)$. [c] Data were taken from references [11] and [25]. n.d. = not determined.

the pyridine nitrogen atom in the *meta* position. Here, the T_m value increases only by 10.0°C (ODN-11-ODN-5; Figure 4c). Most interestingly, such a positional phenomenon was not observed for the corresponding aps duplexes that incorporate PyrdC–PyrdC base pairs of 2 or 3 (Figure 4b,d). Hence, both derivatives show similar stabilities (ODN-10-ODN-3 and ODN-11-ODN-6).

To shed more light on the different strength of silver-mediated PyrdC–PyrdC base pairs in ps DNA, various combinations of hetero base pairs ($^{2\text{py}}\text{PyrdC}$ – $^{3\text{py}}\text{PyrdC}$, $^{\text{ph}}\text{PyrdC}$ – $^{2\text{py}}\text{PyrdC}$, and $^{\text{ph}}\text{PyrdC}$ – $^{3\text{py}}\text{PyrdC}$) were studied in addition to the homo pairs (Table 5). The silver-mediated hetero base pair containing one $^{2\text{py}}\text{PyrdC}$ residue (ODN-2-ODN-11) shows an additional increase in T_m value (ca. $+10^\circ\text{C}$) relative to those base pairs without a $^{2\text{py}}\text{PyrdC}$ residue (ODN-5-ODN-7). In view of this finding, it is anticipated that the pyridine *ortho*-nitrogen atom participates in silver-ion binding, whereas such an interaction does not take place with the nitrogen atom at the *meta* position or in the case of the 6-phenyl derivative 1. In aps DNA, the pyridine residues with the nitrogen atom at *ortho* or *meta* positions show a similar stabilizing effect. Thus, the participation of the pyridine *ortho*-nitrogen atom in silver-ion binding is restricted to ps DNA. Possible structures of silver-mediated PyrdC base pairs are discussed later.

hetero base pairs was next studied. To this end, the stability of duplexes that incorporate PyrdC derivatives 1–3 was determined in the absence and presence of silver ions (Table 5).

The melting experiments demonstrate that ps duplexes that contain homo PyrdC–PyrdC pairs are strongly stabilized by silver ions (Table 5). Such a strong stabilization of ps DNA has not been observed before. The stability increase amounts to 21.0°C for the $^{2\text{py}}\text{PyrdC}$ – $^{2\text{py}}\text{PyrdC}$ homo base pair (ODN-10-ODN-2; see Figure 4a and Table 5). This effect is almost identical to that found in the corresponding duplex with antiparallel-strand orientation (ODN-10-ODN-3; $\Delta T_m = +21.5^\circ\text{C}$). The strong stabilization caused by 2 with the pyridine nitrogen atom in the *ortho* position to the pyrrole linkage is not observed for the $^{3\text{py}}\text{PyrdC}$ – $^{3\text{py}}\text{PyrdC}$ base pair with

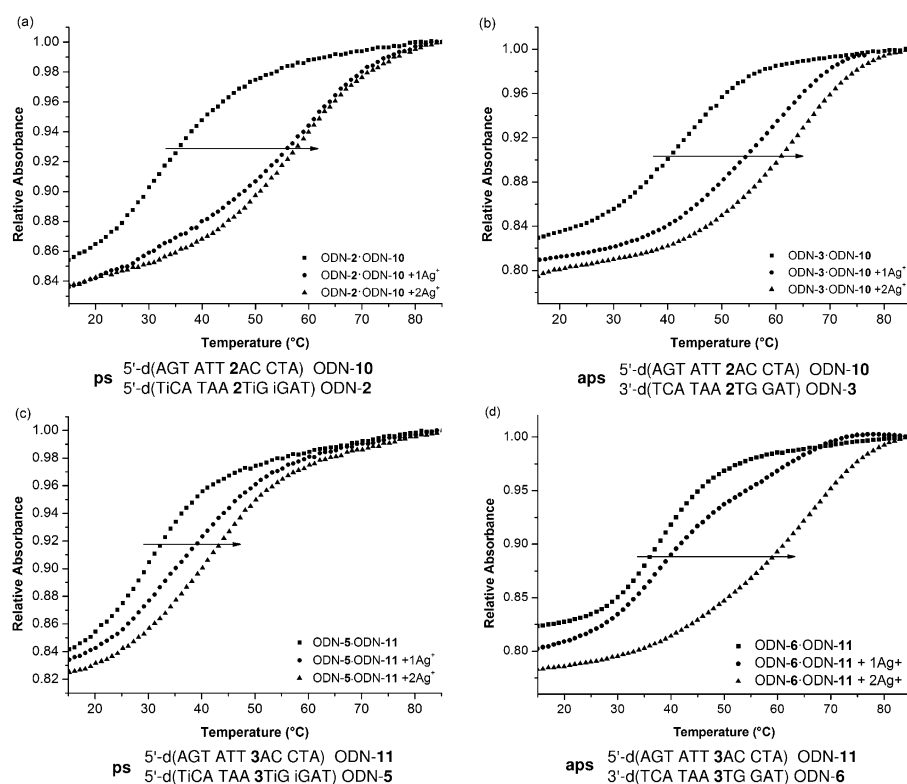


Figure 4. Thermal-denaturation experiments were performed with $5 \mu\text{M}$ duplex in buffer solution (100 mM NaOAc, 10 mM $\text{Mg}(\text{OAc})_2$, pH 7.4) at $\lambda = 260$ nm in the presence of various concentrations of Ag^+ ions (0–2.0 equiv.). a) ps ODN-10-ODN-2; b) aps ODN-10-ODN-3; c) ps ODN-11-ODN-5; d) aps ODN-11-ODN-6. Relative absorbance = A/A_{max} at $\lambda = 260$ nm.

Table 5. T_m values of 12-mer DNA duplexes with PyrdC–PyrdC base pairs in the absence and presence of silver ions.^[a]

| | | T_m [°C] with n equiv of AgNO_3 | | | ΔT_m [°C] ^[b] | ΔT_m [°C] ^[c] |
|--------------------------------------|----------|--|-----------------------|-------|----------------------------------|----------------------------------|
| | | $n=0$ | $n=1$ | $n=2$ | | |
| ps duplexes | | | | | | |
| ps reference duplex | | | | | | |
| 5'-d(TAG GTC AAT ACT) | (ODN-12) | 34.5 | n.d. | 33.5 | −1.0 | − |
| 5'-d(ATC iCAIG TTA TiGA) | (ODN-13) | | | | | |
| PyrdC–PyrdC homo base pairs | | | | | | |
| 5'-d(AGT ATT 1AC CTA) | (ODN-7) | – | – | – | – | – |
| 5'-d(TiCA TAA 1TiG iGAT) | (ODN-8) | | | | | |
| 5'-d(AGT ATT 2AC CTA) | (ODN-10) | 35.0 | – ^[f] / | 56.0 | +21.0 | +21.5 |
| 5'-d(TiCA TAA 2TiG iGAT) | (ODN-2) | | 56.5 ^[d] | | | |
| 5'-d(AGT ATT 3AC CTA) | (ODN-11) | 30.0 | 35.0 | 40.0 | +10.0 | +5.5 |
| 5'-d(TiCA TAA 3TiG iGAT) | (ODN-5) | | | | | |
| PyrdC–PyrdC hetero base pairs | | | | | | |
| 5'-d(AGT ATT 3AC CTA) | (ODN-11) | 31.0 | – ^[f] / | 50.0 | +19.0 | +15.5 |
| 5'-d(TiCA TAA 2TiG iGAT) | (ODN-2) | | 52.0 ^[d] | | | |
| 5'-d(AGT ATT 1AC CTA) | (ODN-7) | 33.0 | – ^[f] / | 47.5 | +14.5 | +13.0 |
| 5'-d(TiCA TAA 2TiG iGAT) | (ODN-2) | | 47.5 ^[d] | | | |
| 5'-d(AGT ATT 1AC CTA) | (ODN-7) | 30.5 | n.d. | 36.0 | +5.5 | +1.5 |
| 5'-d(TiCA TAA 3TiG iGAT) | (ODN-5) | | | | | |
| aps duplexes | | | | | | |
| aps reference duplex | | | | | | |
| 5'-d(AGT ATT GAC CTA) | (ODN-14) | 46.5 | 47.0 | 46.5 | +0 | – |
| 3'-d(TCATAA CTG GAT) | (ODN-15) | | | | | |
| PyrdC–PyrdC homo base pairs | | | | | | |
| 5'-d(AGT ATT 1AC CTA) | (ODN-7) | 35.0 ^[e] | ≈30.0/ | 57.5 | +22.5 ^[e] | +11.0 |
| 3'-d(TCA TAA 1TG GAT) | (ODN-9) | | 58.0 ^[d,e] | | | |
| 5'-d(AGT ATT 2AC CTA) | (ODN-10) | 42.0 ^[e] | 56.0 | 63.5 | +21.5 | +17.0 |
| 3'-d(TCA TAA 2TG GAT) | (ODN-3) | | | | | |
| 5'-d(AGT ATT 3AC CTA) | (ODN-11) | 35.5 | ≈33.0/ | 61.5 | +26.0 | +15.0 |
| 3'-d(TCA TAA 3TG GAT) | (ODN-6) | | 62.0 ^[d] | | | |
| PyrdC–PyrdC hetero base pairs | | | | | | |
| 5'-d(AGT ATT 3AC CTA) | (ODN-11) | 37.5 | n.d. | 64.0 | +26.5 | +17.5 |
| 3'-d(TCA TAA 2TG GAT) | (ODN-3) | | | | | |
| 5'-d(AGT ATT 1AC CTA) | (ODN-7) | 36.5 | n.d. | 62.5 | +26.0 | +16.0 |
| 3'-d(TCA TAA 2TG GAT) | (ODN-3) | | | | | |
| 5'-d(AGT ATT 1AC CTA) | (ODN-7) | 35.0 | n.d. | 62.0 | +27.0 | +15.5 |
| 3'-d(TCA TAA 3TG GAT) | (ODN-6) | | | | | |

[a] Measured at λ_{260} nm with $5 \mu\text{M} + 5 \mu\text{M}$ single-strand concentration at a heating rate of $1.0^\circ\text{C min}^{-1}$ in buffer solution (100 mM NaOAc, 10 mM $\text{Mg}(\text{OAc})_2$, pH 7.4) in the presence of various concentrations of AgNO_3 (0–2.0 equiv.). T_m values were calculated from the heating curves. [b] $\Delta T_m = T_m(\text{after addition of 2 equiv } \text{AgNO}_3) - T_m(\text{before addition of } \text{AgNO}_3)$. [c] $\Delta T_m = T_m(\text{after addition of 2 equiv } \text{AgNO}_3) - T_m(\text{reference ps/aps duplexes})$. [d] Biphasic melting. [e] Data were taken from reference [25]. [f] T_m value cannot be calculated. n.d. = not determined. The structures of iC_d and $meiG_d$ are shown in Table 3.

Stoichiometry of the silver DNA complexes and the proposed silver-mediated PyrdC–PyrdC base pairs

We have demonstrated the high silver-binding affinity of PyrdC–PyrdC homo base pairs in ps duplexes by the extraordinary high thermal stability of the DNA silver complexes (see above). Now, the stoichiometry of the silver ion/PyrdC–PyrdC homo base pair complexes was determined for ps DNA and, for comparison, aps DNA. To this end, UV and fluorescence spectroscopic measurements were performed. In the experi-

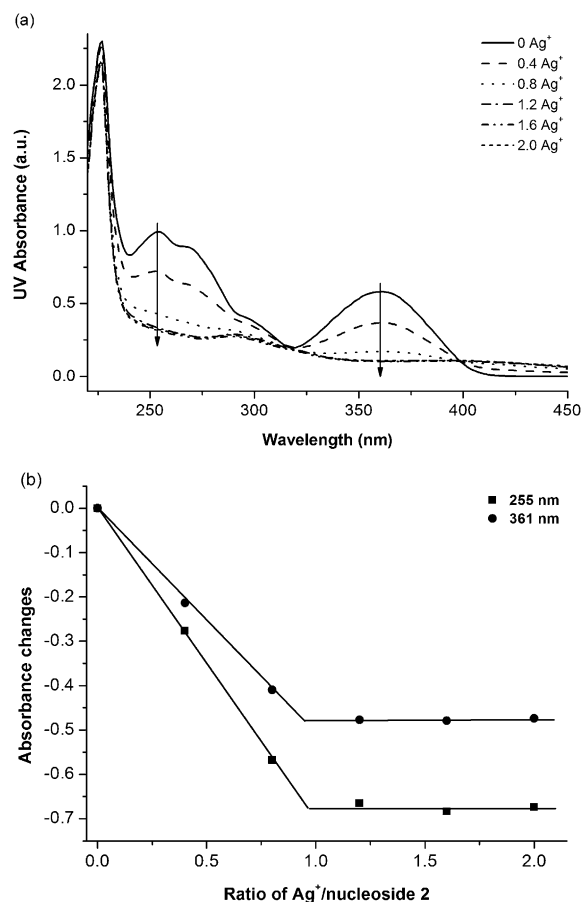


Figure 5. a) UV spectrophotometric titration of $^{2\text{py}}\text{PyrdC}$ ($2; 5 \mu\text{M}$) with increasing concentrations of Ag^+ ions (0.0–2.0 equiv) in buffer solution (100 mM NaOAc, 10 mM $\text{Mg}(\text{OAc})_2$, pH 7.4) containing 0.5% DMSO at 20°C . b) Graphs of the ratio of equivalents of silver ions/nucleoside 2 versus changes in absorbance measured at $\lambda = 255$ and 361 nm.

mental setup, the UV or fluorescence changes were plotted versus the ratio of the silver/duplex concentration. The data were collected at different wavelengths.

Because we anticipated that the silver complexes are already formed by nucleosides 1–3, UV titration experiments were performed at room temperature in the same buffer used for the T_m measurements. The UV absorbance of PyrdC derivatives 1–3 decreases with the addition of silver ions, and the stoichiometric ratio of the PyrdC/silver ion complexes is 1:1, as already anticipated from the melting experiments (see Figure 5 and Figure S5 in the Supporting Information). From that outcome, it is concluded that one molecule of the PyrdC nucleosides 1–3 binds one silver ion or that two silver ions are bound by a pair of PyrdC–PyrdC nucleosides.

UV titration experiments were performed on the duplex ODN-5-ODN-11 with parallel chains (Figure 6a). From the absorbance changes at $\lambda = 258$ and 271 nm the ratio of silver ions/ $^{3\text{py}}\text{PyrdC}$ – $^{3\text{py}}\text{PyrdC}$ base pair could be determined to be 2:1 (Figure 6b).

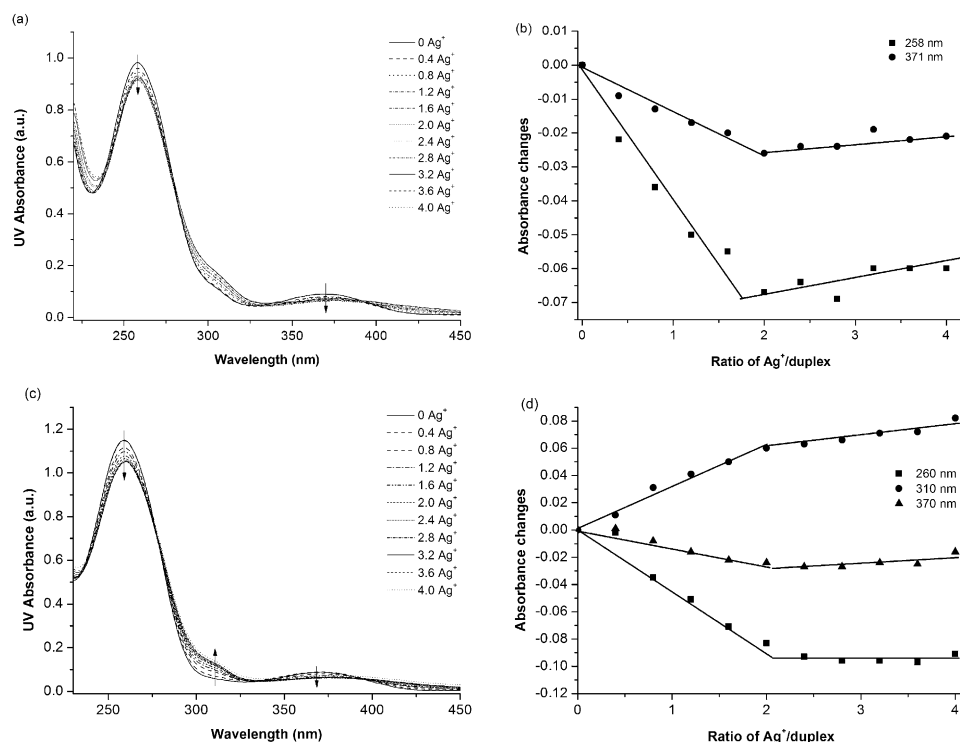


Figure 6. UV spectrophotometric titration of double-stranded DNA ($5 \mu\text{M} + 5 \mu\text{M}$ single-strand oligonucleotide concentration) with increasing concentrations of Ag^+ ions (0.0–4.0 equiv) measured in buffer solution (100 mM NaOAc , 10 mM $\text{Mg}(\text{OAc})_2$, pH 7.4) at 20°C . a) ps ODN-5-ODN-11 and c) aps ODN-6-ODN-11. b, d) Graphs of the ratio of equivalents of silver ions/duplex versus changes in absorbance measured at different wavelengths from (a) and (c), respectively.

We noticed that in the case of ps DNA only small changes in UV absorption occurred during the titration experiments with silver ions, thus making it more difficult to generate a plot of metal binding from which the ratio of silver binding could be determined. This problem was not observed in the case of aps DNA (ODN-6-ODN-11; Figure 6c,d). This difference can be attributed to significant structural differences in ps and aps DNA. The grooves of ps DNA are similar, whereas canonical DNA has a major and a minor groove. Also, the base-pair overlap is different and the phosphodiester backbone of ps DNA seems to be more rigid.^[19] All these properties influence the UV response of silver-ion binding.

In earlier studies, we showed that PyrdC nucleosides can be used as fluorescent probes for silver-ion binding in aps DNA.^[12] Thus, we considered the use of fluorescence titration to determine the stoichiometry of the silver/duplex ratio for ps DNA and to overcome the difficulties observed during UV titration.

In ps duplex ODN-5-ODN-11, which contains a $^3\text{pyPyrdC}$ – $^3\text{pyPyrdC}$ homo base pair, the fluorescence is strongly quenched by the silver ions. By plotting the changes in fluorescence-emission intensity against the ratio of silver/duplex, a defined inflection point is observed from which a 2:1 stoichiometry of silver/ps duplex ODN-5-ODN-11 was determined (Figure 7a,b). The stoichiometry for the homo base pairs of $^2\text{pyPyrdC}$ in the ps duplex DNA was also determined by using this method (see Figure S6 in the Supporting Information). Taken together, our results demonstrate that one PyrdC–PyrdC

homo base pair captures two silver ions in the duplex DNA with parallel-strand orientation. For comparison, the fluorescence-titration experiments were performed with the aps duplex ODN-6-ODN-11 and lead to the same ratio of silver-ion binding (Figure 7c,d). In ps and aps duplexes, the quenching of fluorescence by the addition of silver ions is similar. Based on these findings, fluorescence silver titration experiments can be considered to be a valuable method to study the stoichiometry of metal/base pairs in ps DNA.

Earlier, we proposed structures for silver-mediated $^{\text{ph}}\text{PyrdC}$ – $^{\text{ph}}\text{PyrdC}$ and $^2\text{pyPyrdC}$ – $^2\text{pyPyrdC}$ base pairs in DNA with antiparallel chain orientation.^[11,25] These base pairs were formed by head-to-head alignment of the nucleobases with silver ions bound to N1 and N7 (Figure 8).^[26,27] A similar base pair is now proposed for ps DNA but with the nucleobases in a head-to-tail alignment. As reported before,^[2c] the reverse

Watson–Crick base pairs of dA–dT, iG_d–dC, or $^{\text{me}}\text{rC}_d$ –dG fit well in the ps double helix. The change from a head-to-head arrangement of the silver-mediated PyrdC base pair in aps DNA to a head-to-tail alignment in ps DNA follows the same principle as described for the change of the Watson–Crick base pair in aps DNA to the reverse Watson–Crick pair in ps DNA. A similar change for the silver-mediated dC–dC base pair has been reported by Ono and co-workers^[17a] and also by the computational studies of Marino and co-workers.^[17b]

According to the altered alignment, the nucleobases are now in a different chemical environment with the option for other interactions (Figure 8). Nevertheless, we anticipate that silver ions still interact with N-1 and N-7. However, additional interactions with the pyridine ligands are now possible, which might change the stability of the silver-mediated base pairs.^[28] This assumption is supported by the observation that the silver-mediated $^2\text{pyPyrdC}$ – $^2\text{pyPyrdC}$ base pair is significantly more stable than the $^3\text{pyPyrdC}$ – $^3\text{pyPyrdC}$ pair, thus leading to an increase in T_m value of 21.0°C , a phenomenon that has never been reported before. From this case, it is concluded that the *ortho*-nitrogen atom of the pyridine moiety of $^2\text{pyPyrdC}$ takes part in silver-ion binding, possibly by forming an additional interaction. This situation is in line with the different coordination numbers of the silver ions (2–4)^[29] and can explain the changes in silver-ion binding for the isomeric pyridine residues in silver-mediated PyrdC–PyrdC base pairs.

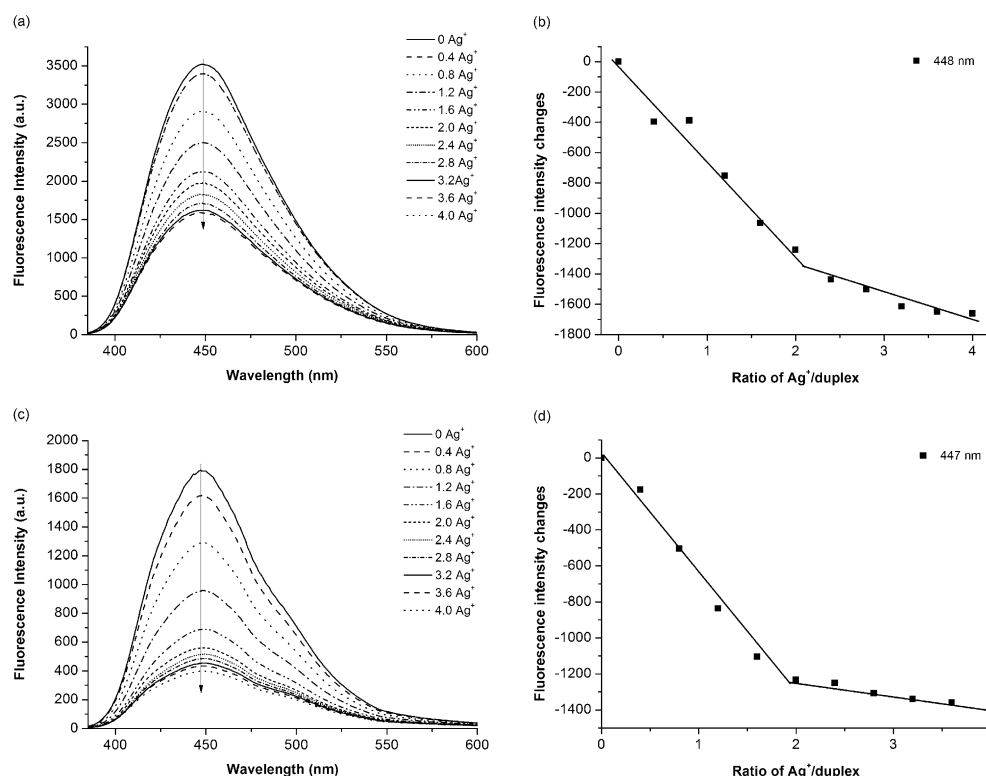
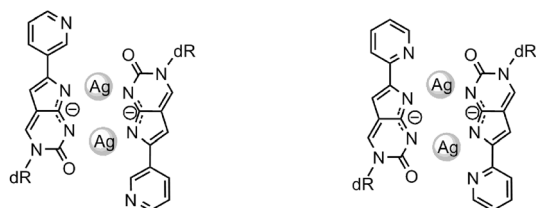


Figure 7. Fluorescence titration of 5 μM double-stranded DNA with increasing concentrations of Ag^+ ions (0.0–4.0 equiv) in buffer solution (100 mM NaOAc, 10 mM Mg(OAc)₂, pH 7.4) at 20 °C. a) ps ODN-5-ODN-11 and c) aps ODN-6-ODN-11. b, d) Graphs of the ratio of equivalents of silver/duplex versus changes in fluorescence measured at $\lambda = 448$ nm from (a) and $\lambda = 447$ nm from (c), respectively.

Such a phenomenon was not observed in aps DNA, in which the replacement of a 6-phenyl by a 6-pyridinyl residue contributes only very little to the stability (+5 °C) and is independent of the position of the nitrogen atom in the pyridine moiety.

Head-to-tail base pairs in ps DNA



Head-to-head base pairs in aps DNA



Figure 8. Proposed silver-mediated PyrdC–PyrdC base pairs in ps DNA and aps DNA. Ag corresponds to Ag^+ .

25-mer duplexes with dA–dT and PyrdC–PyrdC base pairs

Earlier, it was observed by our laboratory that single pyrrolo[2,3-*d*]pyrimidine or pyrazolo[3,4-*d*]pyrimidine residues incorporated in longer ps duplexes (25-mers) had only a small stabilizing effect ($\Delta T_m = +2.0$ – 3.0 °C and $+5.5$ °C for the G-clamp).^[5a,b,6] Because silver-mediated PyrdC–PyrdC base pairs caused already strong stabilization in short 12-mer ps duplexes ($\Delta T_m = +10$ – 20 °C), we reasoned that this phenomenon works also efficiently on longer duplexes that do not contain iG_d and iC_d. Consequently, 1–3 were incorporated into 25-mer oligonucleotides containing only dA–dT and modified PyrdC–PyrdC base pairs, and the impact of silver ions on the duplex stability was investigated. The strand orientation of the resulting duplexes was determined by the sequence motif.^[19] The T_m values obtained in the absence and

presence of silver ions are displayed in Table 6.

One single silver-mediated ^{2py}PyrdC–^{2py}PyrdC base pair causes an enormous stabilization of the ps duplex ODN-18-ODN-19, with an increase in T_m value of 13.5 °C. For comparison, the corresponding aps duplex ODN-18-ODN-25 is only stabilized by 8.5 °C. In the case of the silver-mediated ^{ph}PyrdC–^{ph}PyrdC and ^{3py}PyrdC–^{3py}PyrdC base pairs, a similar increase in T_m value is observed for both duplex orientations. The results of the hybridization experiments of the 25-mer duplexes demonstrate that the silver-mediated ^{2py}PyrdC–^{2py}PyrdC base pair strongly stabilizes ps DNA, independent of the sequence motif.

Because we were surprised by the strong stabilization of ps duplexes by the silver-mediated ^{2py}PyrdC–^{2py}PyrdC base pair, we went back to a recent observation in which aps DNA metal-mediated base pairs were able to reach the stability of a covalent cross-link by changing the molecularity of melting.^[25]

To evaluate this matter for ps DNA, a parallel-stranded cross-linked duplex with an identical sequence to ODN-18-ODN-19 containing a dA–dT base pair instead of the silver-mediated ^{2py}PyrdC–^{2py}PyrdC base pair was designed. Therefore, 25-mer oligonucleotides ODN-14 and ODN-15 were synthesized containing 7-octadiynyl-7-deaza-dA (**A***) and 5-octadiynyl-dU (**U***) in place of dA and dT at the 5'-terminus of the ps duplex (Table 3).^[30] Then, a covalent cross-link was introduced by using “bis-click” ligation with 1,4-bis-azidomethylbenzene (bis-azide) as a cross-linker.

Table 6. T_m values of 25-mer ps and aps DNA duplexes containing PyrdC derivatives in the presence or absence of silver ions.^[a]

| | | T_m [°C] with n equiv of AgNO_3 | | ΔT_m [°C] ^[b] | ΔT_m [°C] ^[c] |
|--|----------|--|-------|----------------------------------|----------------------------------|
| | | $n=0$ | $n=2$ | | |
| ps duplexes | | | | | |
| 5'-d(AAA AAA AAA ATA ATT TTA AAT ATTT) | (ODN-22) | 42.0 | 43.0 | +1.0 | – |
| 5'-d(TTT TTT TTT TAT TAA AAT TTA TAAA) | (ODN-23) | | | | |
| 5'-d(AAA AAA AAA ATA 1TT TTA AAT ATTT) | (ODN-16) | 36.5 | 43.0 | +6.5 | +1.0 |
| 5'-d(TTT TTT TTT TAT 1AA AAT TTA TAAA) | (ODN-17) | | | | |
| 5'-d(AAA AAA AAA ATA 2TT TTA AAT ATTT) | (ODN-18) | 41.0 | 54.5 | +13.5 | +12.5 |
| 5'-d(TTT TTT TTT TAT 2AA AAT TTA TAAA) | (ODN-19) | | | | |
| 5'-d(AAA AAA AAA ATA 3TT TTA AAT ATTT) | (ODN-20) | 38.5 | 45.5 | +7.0 | +3.5 |
| 5'-d(TTT TTT TTT TAT 3AA AAT TTA TAAA) | (ODN-21) | | | | |
| 5'-d(AAA AAA AAA ATA 1TT TTA AAT ATTT) | (ODN-16) | 39.0 | 51.0 | +12.0 | +9.0 |
| 5'-d(TTT TTT TTT TAT 2AA AAT TTA TAAA) | (ODN-19) | | | | |
| 5'-d(AAA AAA AAA ATA 3TT TTA AAT ATTT) | (ODN-20) | 38.0 | 51.0 | +13.0 | +9.0 |
| 5'-d(TTT TTT TTT TAT 2AA AAT TTA TAAA) | (ODN-19) | | | | |
| aps duplexes | | | | | |
| 5'-d(AAA AAA AAA ATA ATT TTA AAT ATTT) | (ODN-22) | 55.0 | 56.5 | +1.5 | – |
| 3'-d(TTT TTT TTT TAT TAA AAT TTA TAAA) | (ODN-27) | | | | |
| 5'-d(AAA AAA AAA ATA 1TT TTA AAT ATTT) | (ODN-16) | 50.5 | 56.0 | +5.5 | +1.0 |
| 3'-d(TTT TTT TTT TAT 1AA AAT TTA TAAA) | (ODN-24) | | | | |
| 5'-d(AAA AAA AAA ATA 2TT TTA AAT ATTT) | (ODN-18) | 52.0 | 60.5 | +8.5 | +5.5 |
| 3'-d(TTT TTT TTT TAT 2AA AAT TTA TAAA) | (ODN-25) | | | | |
| 5'-d(AAA AAA AAA ATA 3TT TTA AAT ATTT) | (ODN-20) | 52.5 | 57.5 | +5.0 | +2.5 |
| 3'-d(TTT TTT TTT TAT 3AA AAT TTA TAAA) | (ODN-26) | | | | |
| 5'-d(AAA AAA AAA ATA 1TT TTA AAT ATTT) | (ODN-16) | 52.0 | 59.5 | +7.5 | +4.5 |
| 3'-d(TTT TTT TTT TAT 2AA AAT TTA TAAA) | (ODN-25) | | | | |
| 5'-d(AAA AAA AAA ATA 3TT TTA AAT ATTT) | (ODN-20) | 51.5 | 61.0 | +9.5 | +6.0 |
| 3'-d(TTT TTT TTT TAT 2AA AAT TTA TAAA) | (ODN-25) | | | | |

[a] Measured at 260 nm with $5\ \mu\text{M} + 5\ \mu\text{M}$ single-strand concentration at a heating rate of $1.0\ ^\circ\text{C min}^{-1}$ in buffer solution (100 mM NaOAc, 10 mM Mg(OAc)₂, pH 7.4) in the presence of various concentrations of AgNO_3 (0–2.0 equiv). T_m values were calculated from the heating curves. [b] $\Delta T_m = T_m(\text{after addition of 2 equiv AgNO}_3) - T_m(\text{before addition of AgNO}_3)$. [c] $\Delta T_m = T_m(\text{after addition of 2 equiv AgNO}_3) - T_m(\text{reference ps/aps duplexes})$.

Based on the template effect of ps duplexes and the flexibility of the terminal residues, only the target heterodimer ODN-28 was obtained. Homodimer formation was not detected. The structure of the ps cross-linked heterodimer was confirmed by mass changes determined by MALDI-TOF mass-spectrometric analysis and ion-exchange HPLC (see Table 3 and Figure S8b; see the Supporting Information for the synthesis).

The ps duplex ODN-18-ODN-19 containing a silver-mediated $^{2\text{py}}\text{PyrdC}$ – $^{2\text{py}}\text{PyrdC}$ base pair shows a similar T_m value to the cross-linked duplex ODN-28 ($T_m = 54.5$ and $56.0\ ^\circ\text{C}$, respectively; see Table 6 and Figure 9). Thus, the silver-mediated $^{2\text{py}}\text{PyrdC}$ – $^{2\text{py}}\text{PyrdC}$ base pair reaches the stability of a covalent interstrand cross-link in ps DNA.

Conclusion

Oligonucleotides (12- and 25-mers) that incorporate the 6-pyridinyl pyrrolo[2,3-*d*]pyrimidine nucleosides $^{2\text{py}}\text{PydC}$ and $^{3\text{py}}\text{PyrdC}$ (2 and 3, respectively) have been synthesized by using solid-phase synthesis that employed phosphoramidite chemistry. Both PyrdC nucleosides developed strong fluorescence with exceptionally high brightness. The fluorescence in the oligonu-

cleotides was sensitive to environmental changes, such as base pairing or silver-ion binding. Stoichiometric UV and fluorescence titration experiments demonstrated that two silver ions were captured by one PyrdC–PyrdC base pair in DNA with parallel-strand orientation. The formation of silver-mediated PyrdC–PyrdC base pairs strongly stabilized the duplex DNA with parallel-chain orientation. Nevertheless, the silver-mediated $^{2\text{py}}\text{PyrdC}$ – $^{2\text{py}}\text{PyrdC}$ (2) base pair was significantly more stable than that of $^{3\text{py}}\text{PyrdC}$ 3. Apparently, only the pyridine nitrogen atom positioned *ortho* to the functionalization site takes part in silver-ion binding by forming an additional coordination. A structure is proposed for the silver-ion/PyrdC base pair in ps DNA, which aligns the nucleobases head-to-tail instead of head-to-head, as suggested for aps DNA. To the best of our knowledge, this example is the first of a dinuclear silver-mediated base pair in a reverse Watson–Crick double helix. With a single silver-mediated $^{2\text{py}}\text{PyrdC}$ – $^{2\text{py}}\text{PyrdC}$ base-pair modification, ps DNA can reach the stability of aps DNA contain-

ing Watson–Crick base pairs. Such a strong stabilization has never been reported before.

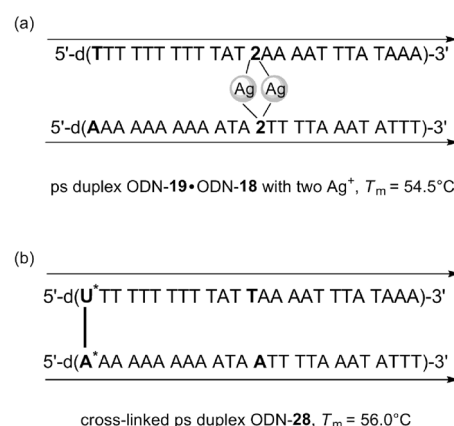


Figure 9. Schematic illustration of a) ps duplex ODN-19-ODN-18 with a silver-mediated $^{2\text{py}}\text{PyrdC}$ – $^{2\text{py}}\text{PyrdC}$ base pair and b) ODN-28 with a covalent cross-link. The structure of the cross-linker d(A*–U*) is shown in Table 3 and the synthesis of ODN-28 by using the “bis-click” reaction is shown in the Supporting Information. Ag corresponds to Ag^+ , 2 = $^{2\text{py}}\text{PyrdC}$.

Experimental Section

General methods and materials

All chemicals and solvents were of laboratory grade as obtained from commercial suppliers and were used without further purification. TLC analysis was performed on TLC aluminium sheets covered with silica gel 60 F254. Flash column chromatography (FC) was carried out on silica gel 60 at 0.4 bar. UV spectra were recorded on a U-3200 UV/Vis spectrometer. ^1H , ^{13}C , and ^{31}P NMR spectra were measured at 300.15 MHz for ^1H , 75.48 MHz for ^{13}C , and 121.52 MHz for ^{31}P , the δ values are given in ppm relative to Me_4Si as an internal standard (^1H and ^{13}C) or external 85% H_3PO_4 (^{31}P). The J values are given in Hz. For NMR spectra measured in $[\text{D}_6]\text{DMSO}$, the chemical shift of the solvent peak was set to $\delta = 2.50$ ppm for ^1H NMR and $\delta = 39.50$ ppm for ^{13}C NMR. DEPT-135 and ^1H - ^{13}C gated-decoupled spectra were used for the assignment of the ^{13}C resonance signals. See Table S1 in the Supporting Information for the ^1H - ^{13}C coupling constants. Reversed-phase HPLC was carried out on a 4 \times 250 mm RP-18 (10 μm) LiChrospher 100 column with a HPLC pump connected with a variable wavelength monitor, a controller, and an integrator. The molecular masses of the oligonucleotides were determined by MALDI-TOF mass-spectrometric analysis in the linear positive mode with 3-hydroxyphenylacetic acid (3-HPA) as a matrix.

The thermal-melting curves were measured on a UV/Vis spectrophotometer equipped with a thermoelectrical controller. The temperature was measured continuously in the reference cell with a Pt-100 resistor with a heating rate of 1°C min^{-1} . The T_m values were determined from the melting curves by using the software MELTWIN, version 3.0.^[31]

Syntheses, purification, and characterization of oligonucleotides containing PyrdC nucleosides

Oligonucleotide syntheses were performed on an ABI 392-08 synthesizer on a scale of 1 μmol scale (trityl-on mode) and employed the standard phosphoramidites and the modified building blocks 10–14 following the synthesis protocol for 3'-O-(2-cyanoethyl)-phosphoramidites. The average coupling yield was always higher than 95%. After cleavage from the solid support, oligonucleotides containing iG_d and iC_d modifications were deprotected in 25% aqueous NH_3 at room temperature for 2 days. Other oligonucleotides were incubated in 25% aqueous NH_3 at 60°C for 1 h and kept overnight at room temperature to accomplish complete deprotection. The DMT-containing oligonucleotides were purified by reversed-phase HPLC (RP-18) with the following solvent gradient system: A: 0.1 M (Et_3NH)OAc (pH 7.2)/MeCN 95:5; B: MeCN; gradient I: 0–3 min 10–15% B in A, 3–15 min 15–50% B in A, 15–20 min 50–10% B in A, flow rate: 0.75 mL min $^{-1}$. The fractions containing oligonucleotides were evaporated to dryness, and the residue was treated with dichloroacetic acid (2.5% in CH_2Cl_2) for 3 min at 0°C to remove the 4,4'-dimethoxytrityl residues. The detritylated oligomers were purified by reversed-phase HPLC with gradient II: 0–20 min 0–20% B in A, 20–25 min 20% B in A, 25–30 min 20–0% B in A, flow rate: 0.75 mL min $^{-1}$. The oligonucleotides were desalted on a short column (RP-18, silica gel) with H_2O for the elution of the salt, while the oligonucleotides were eluted with $\text{MeOH}/\text{H}_2\text{O}$ (3:2). The oligonucleotides were lyophilized on a Speed Vac evaporator to yield colorless solids, which were stored frozen at -24°C . The extinction coefficients ϵ_{260} (mol $^{-1}$ dm 3 cm $^{-1}$ in H_2O) of the nucleosides are dA: 15400, dG: 11700, dT: 8800, dC: 7300, 1: 21000 (MeOH), 2: 19900 (MeOH), and 3: 19200 (MeOH). The extinction

coefficients of the oligonucleotides were calculated from the sum of the extinction coefficients of the nucleoside constituents.

4-Amino-1-(2-deoxy- β -D-erythro-pentofuranosyl)-5-(3-pyridinylethynyl)pyrimidin-2(1H)-one (6): $[\text{Pd}(\text{PPh}_3)_2\text{Cl}_2]$ (250 mg, 0.35 mmol), anhydrous Et_3N (20 mL), and 3-ethynylpyridine (5,^[21] 1.8 g, 16 mmol) were added to a suspension of 5-iodo-2'-deoxycytidine (4,^[16] 2.5 g, 7.1 mmol) and CuI (135 mg, 0.71 mmol) in anhydrous DMF (20 mL). The reaction mixture was heated to reflux in an oil bath and under nitrogen for 4 h. The solvent was removed to afford a gum. Upon the addition of CH_2Cl_2 (100 mL) to the gummy residue, crude **6** precipitated as brown solid (2.3 g, 97% crude yield). This crude product was directly used for the next step. An analytic sample of **6** was purified by FC (silica gel, column 15 \times 3 cm, $\text{CH}_2\text{Cl}_2/\text{MeOH}$, 8:1). $R_f = 0.2$ ($\text{CH}_2\text{Cl}_2/\text{MeOH}$, 10:1); ^1H NMR (300 MHz, $[\text{D}_6]\text{DMSO}$, 25°C): $\delta = 1.99$ –2.08 (m, 1H; 2'-H_a), 2.15–2.21 (m, 1H; 2'-H_b), 3.55–3.69 (m, 2H; 2 \times 5'-H), 3.79–3.82 (m, 1H; 4'-H), 4.20–4.24 (m, 1H; 3'-H), 5.14 (t, $^3J(\text{H,H}) = 4.8$ Hz, 1H; 5'-OH), 5.24 (d, $^3J(\text{H,H}) = 4.2$ Hz, 1H; 3'-OH), 6.12 (t, $^3J(\text{H,H}) = 6.3$ Hz, 1H; 1'-H), 7.15 (brs, 1H; NH_a), 7.42–7.46 (m, 1H; pyridinyl-H), 7.83 (brs, 1H; NH_b), 7.97–8.01 (m, 1H; pyridinyl-H), 8.38 (s, 1H; H-6), 8.53–8.54 (m, 1H; pyridinyl-H), 8.77 ppm (s, 1H; pyridinyl-H); UV/Vis (MeOH): λ_{max} (ϵ) = 310 nm (19900 mol $^{-1}$ dm 3 cm $^{-1}$); MS (ESI): m/z calcd for $\text{C}_{16}\text{H}_{16}\text{N}_4\text{O}_4$: 351.1069; found: 351.1057 [$M + \text{Na}$] $^+$.

4-Amino-1-[2-deoxy-5-O-(4,4'-dimethoxytrityl)- β -D-erythro-pentofuranosyl]-5-(3-pyridinylethynyl)pyrimidin-2(1H)-one (7): Compound **6** (0.97 g, 2.95 mmol) was coevaporated with anhydrous pyridine (2 \times 20 mL) and then dissolved in anhydrous pyridine (15 mL). *N,N*-Diisopropylethylamine (1.5 mL) and then 4,4'-dimethoxytrityl chloride (1.5 g, 4.43 mmol) were added to the reaction mixture, which was kept stirring at room temperature for 8 h. Methanol (2 mL) was added to quench the reaction. The mixture was stirred for another 10 min, diluted with CH_2Cl_2 (160 mL), and extracted with 5% aqueous NaHCO_3 solution (100 mL) followed by H_2O (80 mL). The organic layer was dried over Na_2SO_4 and then concentrated. Purification by FC (silica gel, column 15 \times 3 cm, $\text{CH}_2\text{Cl}_2/\text{MeOH}/\text{Et}_3\text{N}$, 20:1:0.05) provided **7** as white solid (1.32 g, 70%). $R_f = 0.3$ ($\text{CH}_2\text{Cl}_2/\text{MeOH}$, 10:1); ^1H NMR (300 MHz, $[\text{D}_6]\text{DMSO}$, 25°C): $\delta = 2.11$ –2.20 (m, 1H; 2'-H_a), 2.29–2.33 (m, 1H; 2'-H_b), 3.19 (s, 2H; 2 \times 5'-H), 3.64 (s, 6H; 2 \times OCH₃), 3.97–3.98 (m, 1H; 4'-H), 4.31 (m, 1H; 3'-H), 5.33 (brs, 1H; 3'-OH), 6.15 (t, $^3J(\text{H,H}) = 6.3$ Hz, 1H; 1'-H), 6.82–6.86 (m, 4H; DMT-H), 7.12–7.19 (m, 2H; NH_a, DMT-H), 7.25–7.44 (m, 9H; DMT-H, pyridinyl-H), 7.53–7.55 (m, 1H; pyridinyl-H), 7.89 (brs, 1H; NH_b), 8.19 (s, 1H; pyridinyl-H), 8.38 (s, 1H; H-6), 8.46–8.48 ppm (m, 1H; pyridinyl-H); λ_{max} (ϵ) = 232 (39000), 276 (17900), 283 (17800), 312 nm (17900 mol $^{-1}$ dm 3 cm $^{-1}$); MS (ESI): m/z calcd for $\text{C}_{37}\text{H}_{34}\text{N}_4\text{O}_6$: 653.2376; found: 653.2371 [$M + \text{Na}$] $^+$.

4-Acetylamino-1-[2-deoxy-5-O-(4,4'-dimethoxytrityl)- β -D-erythro-pentofuranosyl]-5-(3-pyridinylethynyl)pyrimidin-2(1H)-one (8): Acetic anhydride (90 μL , 0.96 mmol) was added to a solution of **7** (200 mg, 0.32 mmol) in dry DMF (3 mL). The reaction mixture was kept stirring overnight at room temperature, diluted with CH_2Cl_2 (20 mL), and washed with NaHCO_3 (1% aq., 2 \times 20 mL) followed by H_2O (20 mL). The organic layer was dried over Na_2SO_4 and concentrated. Pure product **8** was obtained by FC (silica gel, column 15 \times 3 cm, $\text{CH}_2\text{Cl}_2/\text{MeOH}/\text{Et}_3\text{N}$, 40:1:0.05) as a white solid (130 mg, 61%). $R_f = 0.6$ ($\text{CH}_2\text{Cl}_2/\text{MeOH}$, 10:1); ^1H NMR (300 MHz, $[\text{D}_6]\text{DMSO}$, 25°C): $\delta = 2.24$ –2.31 (m, 4H; 2'-H_a, CH₃), 2.37–2.48 (m, 1H; 2'-H_b), 3.15–3.25 (m, 2H; 2 \times 5'-H), 3.63 (s, 6H; 2 \times OCH₃), 4.05 (m, 1H; 4'-H), 4.30 (m, 1H; 3'-H), 5.37 (d, $^3J(\text{H,H}) = 4.5$ Hz, 1H; 3'-OH), 6.08 (t, $^3J(\text{H,H}) = 6.3$ Hz, 1H; 1'-H), 6.80–6.84 (m, 4H; DMT-H), 7.10–7.45 (m, 11H; DMT-H, pyridinyl-H), 8.29 (m, 1H; pyridinyl-H), 8.46–8.49 (m, 2H; pyridinyl-H, H-6), 9.95 ppm (brs, 1H; NH); λ_{max} (ϵ) = 234

(40200), 283 (19500), 298 nm ($19800 \text{ mol}^{-1} \text{ dm}^3 \text{ cm}^{-1}$); MS (ESI): m/z calcd for $\text{C}_{39}\text{H}_{36}\text{N}_4\text{O}_7$: 695.2482; found: 695.2457 $[\text{M} + \text{Na}]^+$.

6-(3-Pyridinyl)-3-[2-deoxy-5-O-(4,4'-dimethoxytrityl)- β -D-erythro-pentofuranosyl]pyrrolo[2,3-d]pyrimidin-2(3H)-one (9): A mixture of **8** (100 mg, 0.15 mmol), CuI (42.5 mg, 0.22 mmol) in Et_3N (3 mL), and DMF (3 mL) was heated at 60°C for 24 h under nitrogen. The solvent was evaporated and the remaining residue was dissolved in CH_2Cl_2 (30 mL). The organic phase was washed several times with 5% ethylenediaminetetraacetic acid, disodium salt (Na_2EDTA) solution ($4 \times 30 \text{ mL}$), dried over Na_2SO_4 , and evaporated to dryness. The residue was purified by FC (silica gel, column $10 \times 3 \text{ cm}$, $\text{CH}_2\text{Cl}_2/\text{MeOH}/\text{Et}_3\text{N}$, 20:1:0.05) to afford **9** as a light-yellow solid (51 mg, 54%). $R_f = 0.5$ ($\text{CH}_2\text{Cl}_2/\text{MeOH}$, 9:1); ^1H NMR (300 MHz, $[\text{D}_6]\text{DMSO}$, 25°C): $\delta = 2.15\text{--}2.21$ (m, 1H; $2'\text{-H}_\text{a}$), 2.38–2.44 (m, 1H; $2'\text{-H}_\text{b}$), 3.26–3.40 (m, 2H; $5'\text{-H}$ imposed by DMSO), 3.67 (s, 3H; OCH_3), 3.68 (s, 3H; OCH_3), 3.97–3.98 (m, 1H; $4'\text{-H}$), 4.39–4.43 (m, 1H; $3'\text{-H}$), 5.41 (d, $^3J(\text{H,H}) = 4.8 \text{ Hz}$, 1H; $3'\text{-OH}$), 5.97 (s, 1H; $\text{H-1}'$), 6.21 (t, $^3J(\text{H,H}) = 5.5 \text{ Hz}$, 1H; 7-H), 6.91 (m, 4H; DMT-H), 7.22–7.49 (m, 10H; DMT-H, pyridinyl-H), 8.02–8.04 (m, 1H; pyridinyl-H), 8.49–8.50 (m, 1H; pyridinyl-H), 8.66 (s, 1H; 6-H), 8.89–8.90 (m, 1H; pyridinyl-H), 11.90 ppm (brs, 1H; NH); λ_{max} (ϵ) = 234 (38600), 270 (21800), 366 nm ($12100 \text{ mol}^{-1} \text{ dm}^3 \text{ cm}^{-1}$); MS (ESI): m/z calcd for $\text{C}_{37}\text{H}_{34}\text{N}_4\text{O}_6$: 653.2376; found: 653.2365 $[\text{M} + \text{Na}]^+$.

6-(3-Pyridinyl)-3-[2-deoxy-5-O-(4,4'-dimethoxytriphenylmethyl)- β -D-erythro-pentofuranosyl]pyrrolo[2,3-d]pyrimidin-2(3H)-one 3'-(2-cyanoethyl)-N,N-diisopropyl phosphoramidite (10): A stirred solution of **9** (0.46 g, 0.72 mmol) in anhydrous CH_2Cl_2 (10 mL) was treated with $(i\text{Pr})_2\text{NEt}$ (200 μL , 1.14 mmol) followed by 2-cyanoethyl-N,N-diisopropylphosphoramidochloridite (270 μL , 1.22 mmol). After stirring for 45 min at room temperature, the solution was diluted with CH_2Cl_2 (40 mL) and extracted with 5% aqueous NaHCO_3 solution (30 mL) and H_2O (30 mL). The organic layer was dried over Na_2SO_4 and evaporated. The residue was purified by FC (silica gel, column $10 \times 2 \text{ cm}$, $\text{CH}_2\text{Cl}_2/\text{MeOH}/\text{Et}_3\text{N}$, 20:1:0.05) to give **10** as a light-yellow foam (410 mg, 68%). $R_f = 0.2$ ($\text{CH}_2\text{Cl}_2/\text{MeOH}/\text{Et}_3\text{N}$, 25:1:0.05); ^{31}P NMR (121 MHz, CDCl_3 , 25°C): $\delta = 148.9$, 149.7 ppm; MS (ESI): m/z calcd for $\text{C}_{46}\text{H}_{51}\text{N}_6\text{O}_7\text{P}$: 853.3449; found: 853.3439 $[\text{M} + \text{Na}]^+$.

6-(3-Pyridinyl)-3-[2-deoxy- β -D-erythro-pentofuranosyl]pyrrolo[2,3-d]pyrimidin-2(3H)-one (3): A solution of **9** (190 mg, 0.30 mmol) in CH_2Cl_2 (5 mL) was cooled to 0°C in an ice bath. Dichloroacetic acid in dry CH_2Cl_2 (4 mL) was added. The reaction mixture was stirred at 0°C for 40 min and neutralized with triethylamine (3 mL). The solvent was removed under vacuum and the remaining residue was purified by FC (silica gel, column $10 \times 3 \text{ cm}$, $\text{CH}_2\text{Cl}_2/\text{MeOH}$, 9:1–6:1) to afford **3** as a slightly yellow solid (70 mg, 70%). $R_f = 0.4$ ($\text{CH}_2\text{Cl}_2/\text{MeOH}$, 4:1); ^1H NMR (300 MHz, $[\text{D}_6]\text{DMSO}$, 25°C): $\delta = 2.06\text{--}2.09$ (m, 1H; $2'\text{-H}_\text{a}$), 2.34–2.42 (m, 1H; $2'\text{-H}_\text{b}$), 3.60–3.74 (m, 2H; $2 \times 5'\text{-H}$), 3.90–3.93 (m, 1H; $4'\text{-H}$), 4.23–4.27 (m, 1H; $3'\text{-H}$), 5.17 (t, $^3J(\text{H,H}) = 5.1 \text{ Hz}$, 1H; $5'\text{-OH}$), 5.28 (d, $^3J(\text{H,H}) = 4.2 \text{ Hz}$, 1H; $3'\text{-OH}$), 6.25 (t, $^3J(\text{H,H}) = 6.3 \text{ Hz}$, 1H; $1'\text{-H}$), 6.90 (s, 1H; 5-H), 7.45–7.49 (m, 1H; pyridinyl-H), 8.20 (dd, $^3J(\text{H,H}) = 8.1 \text{ Hz}$, $^4J(\text{H,H}) = 1.5 \text{ Hz}$, 1H; pyridinyl-H), 8.52 (d, $^3J(\text{H,H}) = 4.2 \text{ Hz}$, 1H; pyridinyl-H), 8.78 (s, 1H; pyridinyl-H), 9.06 (s, 1H; 6-H), 11.92 ppm (brs, 1H; NH); λ_{max} (ϵ) = 248 (26700), 260 (19200), 364 nm ($13500 \text{ mol}^{-1} \text{ dm}^3 \text{ cm}^{-1}$); MS (ESI): m/z calcd for $\text{C}_{16}\text{H}_{16}\text{N}_4\text{O}_4$: 351.1069; found: 351.1064 $[\text{M} + \text{Na}]^+$.

Acknowledgements

We thank Mr. N.Q. Tran for the oligonucleotide synthesis and Dr. H. Letzel (Organisch-chemisches Institut, Universität Mün-

ster, Germany) for measurement of the MALDI-TOF mass spectra. We also thank Dr. P. Leonard and Dr. S. Budow-Busse for their continuous support throughout the preparation of this manuscript. Financial support by ChemBiotech, Münster, Germany is highly appreciated.

Keywords: chain structures • DNA structures • nitrogen heterocycles • nucleosides • silver

- [1] J. D. Watson, F. H. C. Crick, *Nature* **1953**, 171, 737–738.
- [2] a) F. Geinguenau, J. A. Mondragon-Sanchez, J. Liquier, A. K. Shchylkina, R. Klement, D. J. Arndt-Jovin, T. M. Jovin, E. Taillandier, *Spectrochim. Acta Part A* **2005**, 61, 579–587; b) H. Sugiyama, S. Ikeda, I. Saito, *J. Am. Chem. Soc.* **1996**, 118, 9994–9995; c) F. Seela, Y. He, C. Wei, *Tetrahedron* **1999**, 55, 9481–9500.
- [3] a) F. Seela, Y. He in *Organic and Bioorganic Chemistry*, (Ed.: D. Loakes), Transworld Research Network, Kerala, India, **2002**, "Modified Nucleosides, Synthesis and Applications" on pp. 57–85; b) H. Mei, S. Budow, F. Seela, *Biomacromolecules* **2012**, 13, 4196–4204; c) F. Seela, C. Wei, A. Melewnski, Y. He, R. Kröschel, E. Feiling, *Nucleosides Nucleotides* **1999**, 18, 1543–1548.
- [4] a) K. Rippe, V. Fritsch, E. Westhof, T. M. Jovin, *EMBO J.* **1992**, 11, 3777–3786; b) J. Marfurt, C. Leumann, *Angew. Chem. Int. Ed.* **1998**, 37, 175–177; *Angew. Chem.* **1998**, 110, 184–187; c) V. N. Soyfer, V. N. Potaman, *Triple-Helical Nucleic Acids*, Springer, New York, **1996**; d) H. Fritzsche, A. Akhebat, E. Taillandier, K. Rippe, T. M. Jovin, *Nucleic Acids Res.* **1993**, 21, 5085–5091; e) A. K. Shchylkina, O. F. Borisova, M. A. Livshits, T. M. Jovin, *Mol. Biol.* **2003**, 37, 223–231; f) A. K. Jain, S. Bhattacharya, *Bioconjugate Chem.* **2010**, 21, 1389–1403.
- [5] a) F. Seela, C. Wei, G. Becher, M. Zulauf, P. Leonard, *Bioorg. Med. Chem. Lett.* **2000**, 10, 289–292; b) F. Seela, X. Peng, H. Li, *J. Am. Chem. Soc.* **2005**, 127, 7739–7751.
- [6] X. Ming, P. Ding, P. Leonard, S. Budow, F. Seela, *Org. Biomol. Chem.* **2012**, 10, 1861–1869.
- [7] S. S. Pujari, F. Seela, *J. Org. Chem.* **2013**, 78, 8545–8561.
- [8] a) H. Yang, K. L. Mettera, H. F. Sleiman, *Coord. Chem. Rev.* **2010**, 254, 2403–2415; b) J. Richter, *Physica E* **2003**, 16, 157–173; c) J. K. Barton, E. D. Olmon, P. A. Sontz, *Coord. Chem. Rev.* **2011**, 255, 619–634.
- [9] a) Y. Takezawa, M. Shionoya, *Acc. Chem. Res.* **2012**, 45, 2066–2076; b) G. H. Clever, M. Shionoya, *Coord. Chem. Rev.* **2010**, 254, 2391–2402; c) G. H. Clever, C. Kaul, T. Carell, *Angew. Chem. Int. Ed.* **2007**, 46, 6226–6236; *Angew. Chem.* **2007**, 119, 6340–6350; d) A. Ono, H. Torigoe, Y. Tanaka, I. Okamoto, *Chem. Soc. Rev.* **2011**, 40, 5855–5866; e) S. Taherpour, O. Golubev, T. Lönnberg, *J. Org. Chem.* **2014**, 79, 8990–8999.
- [10] a) H. Inoue, A. Imura, E. Ohtsuka, *Nippon Teitai Kenkyukai Kaishi* **1987**, 7, 1214–1220; b) F. Seela, S. Budow, X. Peng, *Curr. Org. Chem.* **2012**, 16, 161–223.
- [11] H. Mei, I. Röhl, F. Seela, *J. Org. Chem.* **2013**, 78, 9457–9463.
- [12] H. Mei, H. Yang, I. Röhl, F. Seela, *ChemPlusChem* **2014**, 79, 914–918.
- [13] a) A. S. Wahba, A. Esmaili, M. J. Damha, R. H. E. Hudson, *Nucleic Acids Res.* **2010**, 38, 1048–1056; b) A. S. Wahba, F. Azizi, G. F. Deleavay, C. Brown, F. Robert, M. Carrier, A. Kalota, A. M. Gewirtz, J. Pelletier, R. H. E. Hudson, M. J. Damha, *ACS Chem. Biol.* **2011**, 6, 912–919; c) C. Liu, C. T. Martin, *J. Mol. Biol.* **2001**, 308, 465–475; d) F. Wojciechowski, R. H. E. Hudson, *J. Am. Chem. Soc.* **2008**, 130, 12574–12575; e) C. M. Zhang, C. Liu, T. Christian, H. Gamper, J. Rozenski, D. Pan, J. B. Randolph, E. Wickstrom, B. S. Cooperman, Y.-M. Hou, *RNA* **2008**, 14, 2245–2253.
- [14] X. Ming, F. Seela, *Chem. Eur. J.* **2012**, 18, 9590–9600.
- [15] K. S. Park, J. Y. Lee, H. G. Park, *Chem. Commun.* **2012**, 48, 4549–4551.
- [16] M. S. Noé, A. C. Rios, Y. Tor, *Org. Lett.* **2012**, 14, 3150–3153.
- [17] a) T. Ono, K. Yoshida, Y. Saotome, R. Sakabe, I. Okamoto, A. Ono, *Chem. Commun.* **2011**, 47, 1542–1544; b) M. Fortino, T. Marino, N. Russo, *J. Phys. Chem. A* **2014**, DOI: 10.1021/jp5096739.
- [18] I. Sinha, C. F. Guerra, J. Müller, *Angew. Chem. Int. Ed.* **2015**, 54, 3603–3606; *Angew. Chem.* **2015**, 127, 3674–3677.
- [19] a) X. L. Yang, H. Sugiyama, S. Ikeda, I. Saito, A. H.-J. Wang, *Biophys. J.* **1998**, 75, 1163–1171; b) N. B. Ramsing, T. M. Jovin, *Nucleic Acids Res.* **1988**, 16, 6659–6676; c) E. Cubero, F. J. Luque, M. Orozco, *J. Am. Chem.*

- Soc. **2001**, 123, 12018–12025; d) P. S. Pallan, P. Lubini, M. Bolli, M. Egli, *Nucleic Acids Res.* **2007**, 35, 6611–6624.
- [20] P. K. Chang, A. D. Welch, *J. Med. Chem.* **1963**, 6, 428–430.
- [21] B. T. Holmes, W. T. Pennington, T. W. Hanks, *Synth. Commun.* **2003**, 33, 2447–2461.
- [22] R. H. E. Hudson, A. Ghorbani-Choghamarani, *Synlett* **2007**, 6, 0870–0873.
- [23] a) L. M. Wilhelmsson, *Q. Rev. Biophys.* **2010**, 43, 159–183; b) R. W. Sinkeldam, N. J. Greco, Y. Tor, *Chem. Rev.* **2010**, 110, 2579–2619.
- [24] S. J. O. Hardman, S. W. Botchway, K. C. Thompson, *Photochem. Photobiol.* **2008**, 84, 1473–1479.
- [25] H. Mei, S. A. Ingale, F. Seela, *Chem. Eur. J.* **2014**, 20, 16248–16257.
- [26] J. A. R. Navarro, M. A. Romero, J. M. Salas, R. Faure, X. Solans, *J. Chem. Soc. Dalton Trans.* **1997**, 2321–2326.
- [27] J. A. R. Navarro, J. M. Salas, M. A. Romero, R. Faure, *J. Chem. Soc. Dalton Trans.* **1998**, 901–904.
- [28] a) K. Tanaka, Y. Yamada, M. Shionoya, *J. Am. Chem. Soc.* **2002**, 124, 8802–8803; b) J. Hamblin, A. Jackson, N. W. Alcock, M. J. Hannon, *J. Chem. Soc. Dalton Trans.* **2002**, 1635–1641; c) P. Ovejero, E. Asensio, J. V. Heras, J. A. Campo, M. Cano, M. R. Torres, C. Núñez, C. Lodeiro, *Dalton Trans.* **2013**, 42, 2107–2120; d) T. Richters, J. Müller, *Eur. J. Inorg. Chem.* **2014**, 437–441.
- [29] H. Wu, Y. Zhang, C. Chen, J. Zhang, Y. Bai, F. Shi, X. Wang, *New J. Chem.* **2014**, 38, 3688–3698.
- [30] S. S. Pujari, P. Leonard, F. Seela, *J. Org. Chem.* **2014**, 79, 4423–4437.
- [31] J. A. McDowell, D. H. Turner, *Biochemistry* **1996**, 35, 14077–14089.
- [32] V. R. Parvathy, S. R. Bhaumik, K. V. R. Chary, G. Govil, K. Liu, F. B. Howard, H. T. Miles, *Nucleic Acids Res.* **2002**, 30, 1500–1511.
- [33] K. Petrovec, B. J. Ravoo, J. Müller, *Chem. Commun.* **2012**, 48, 11844–11846.

Received: February 11, 2015


Published online on ■ ■ ■, 0000

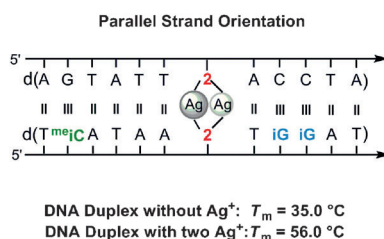
FULL PAPER

DNA Structures

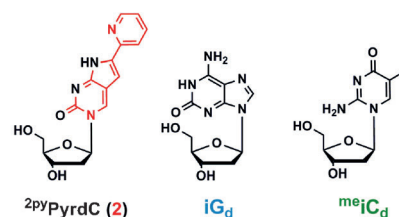
H. Yang, H. Mei, F. Seela*



 **Pyrrolo-dC Metal-Mediated Base Pairs in the Reverse Watson–Crick Double Helix: Enhanced Stability of Parallel DNA and Impact of 6-Pyridinyl Residues on Fluorescence and Silver-Ion Binding**



Base pairs in reverse mode: The highly fluorescent pyrrolo[2,3-*d*]pyrimidine 2'-deoxyribonucleoside (²pyPyrdC, **2**) forms a tremendously stable silver-mediated base pair that incorporates two silver ions in the parallel-stranded



double helix (see picture; dA = 2'-deoxyadenosine, dC = 2'-deoxycytidine, dG = 2'-deoxyguanosine, dT = 2'-deoxythymidine, meiC_d = 5-methyl-2'-deoxyisocytidine, iG_d = 2'-deoxyisoguanosine, T_m = melting temperature).